A BI-CUBIC TRANSFORMATION FOR THE NUMERICAL EVALUATION OF THE CAUCHY PRINCIPAL VALUE INTEGRALS IN BOUNDARY METHODS

M. CERROLAZA

E. ALARCON

INTRODUCTION

It is now widely accepted that the boundary element method has become a powerful tool in the solution of practical problems in engineering. So, during the last decade, a great number of publications and much research has appeared on the subject with regards to both the theoretical aspects as well as the practical applications.[4, 9, 10, 19]

Recently, it has been shown how self-adaptive techniques can be successfully applied within the BEM context.[1, 2, 6, 7, 21, 24, 25] However, although the numerical results are certainly spectacular, it has been found that the poor accuracy in the numerical evaluation of both the nearly singular kernels and the singular ones (i.e. those which exist only in the Cauchy principal value (CPV) sense) is a problem which still remains in the BEM. This lack of accuracy especially affects the BEM *p*-adaptive version, since the macro-elements used to discretize the boundary are chosen as large as possible, provided they do not violate the requirements imposed by the geometry and the boundary conditions.

Furthermore, the evaluation of the residual function in the *p*-version, necessary for the determination of error parameters which govern the refinement process,[2, 5, 7, 8, 12] is a subject that requires the greatest accuracy in the calculation of the variables involved, in order to obtain a reliable refinement criterion.

In the case of nearly singular integrals (i.e. when the source point closely approaches the interval of integration), some special precautions must be taken. Various schemes have been proposed in the technical literature. Jun *et al.*[15] subdivide the interval of integration at the regions close to the source point and then perform the integration in each subdivision by means of standard Gauss–Legendre quadratures. In another publication,[16] these authors employ a double-exponential formula combined with standard Gauss quadratures in order to integrate the nearly singular kernels. These techniques, however, are expensive since they require the use of a high number of sampling points to produce acceptable results. In his interesting paper, Telles[27] presents a non-linear co-ordinate transformation which conveniently gathers the sampling points nearby the source point, thus giving great accuracy. This scheme is very attractive owing to the simplicity of the expressions developed, and it works well enough when evaluating the state of stresses at points placed very close to the boundary.

In the case of singular kernels existing in the CPV sense (i.e. those in which the source point belongs to the interval of integration), one must proceed carefully when performing its evaluation. Some authors, such as Rank[23,24] and Parreira,[21] have employed analytical integration over straight boundary elements. In the *p*-adaptive BEM version, however, such a technique is inadvisable since it notably reduces the possibility of selecting curved macro-elements which must fit large regions of the boundary under consideration.

The numerical quadratures developed by Kutt[17,18] (finite-part quadratures) can also be used, but they need an element subdivision and are not applicable in the presence of singularities of order $O(\log x)$.

It is also possible to use the so-called 'bootstrap' techniques,[22] recently applied to the BEM by Guiggiani and Casalini.[13] These techniques remove the singularity in the following way:

$$\int_a^b \frac{f(x)}{x-\lambda}\,dx = \int_a^b \frac{f(x)-f(\lambda)}{x-\lambda}\,dx + f(\lambda)\int_a^b \frac{dx}{x-\lambda}$$

$$= \int_a^b \frac{f(x)-f(\lambda)}{x-\lambda}\,dx + f(\lambda)\log\left|\frac{b-\lambda}{\lambda-a}\right|$$

where $f(x)$ is a regular function in $[a, b]$, $\lambda \in (a, b)$ and now the integral is regular, so it becomes possible to integrate it by means of standard Gauss–Legendre quadratures, provided that no sampling point coincides with the singular point λ. Nevertheless, these techniques have the disadvantage of not being applicable in the presence of singularities $O(\log x)$ and $O(1/x^{\alpha})$ with $\alpha > 1$.

The aim of this paper is to develop a fully numerical procedure to evaluate both the singular kernels existing in the CPV sense and those containing singularities $O(\log x)$ which normally arise in boundary methods. In what follows, a brief summary of the BEM basic formulae will be included. The proposed numerical method will then be developed in detail. Also, with the purpose of evaluating the accuracy and stability of the numerical procedure, some illustrative examples will be included and discussed.

BRIEF SUMMARY OF BEM FORMULAE

As is well known, the so-called 'direct approach' in the BEM may be stated through the Somigliana integral identity,[4] which is written as (ignoring body forces)

$$\mathbf{C}(P)\cdot\mathbf{u}(P) + \int_\Gamma \mathbf{T}^*(P, Q)\cdot\mathbf{u}(Q)\,d\Gamma(Q) = \int_\Gamma \mathbf{U}^*(P, Q)\cdot\mathbf{t}(Q)\,d\Gamma(Q) \tag{1}$$

The above expression shows the reciprocity relationship between the present state of tractions $\mathbf{t}(Q)$ and displacements $\mathbf{u}(Q)$ at a point $Q \in \Gamma$ and a fundamental solution defined by a unitary concentrated load tensor applied at a point $P \in \Gamma$, whose mechanical state is reflected by both the tractions $\mathbf{T}^*(P, Q)$ and the displacements $\mathbf{U}^*(P, Q)$. $\mathbf{C}(P)$ is a matrix related to the local geometric properties of the surface around the source point P.[14]

If the functions $\mathbf{T}^*(P, Q)$ and $\mathbf{U}^*(P, Q)$ are interpreted in the sense of weighting functions then it will be possible to interpolate $\mathbf{u}(Q)$ and $\mathbf{t}(Q)$ via the classical approach of well-known projective methods, in order to discretize the problem in a set of linear equations

$$\mathbf{A} \cdot \mathbf{X} = \mathbf{F} \tag{2}$$

where $\mathbf{X}$ collects the boundary unknowns and $\mathbf{A}$ and $\mathbf{F}$ are computed through numerical integration of the influence coefficients. The reader interested in the details of the formulae may see, for instance, References 4, 9 and 19.

In the bi-dimensional elastostatics case, the vectorial functions $\mathbf{T}^*(P, Q)$ and $\mathbf{U}^*(P, Q)$ contain singularities of order $O(1/x)$ and $O(\log x)$, respectively. The former is hardly integrable in the CPV sense, while the integration of the second must be performed by splitting the singular kernel and then applying special quadratures with logarithmic weighting functions (see, e.g. Berthold-Zaborowsky[3]). It is clear that the aforementioned procedure implies a certain number of added numerical and computational complications.

On the other hand, the macro-elements selected to discretize the boundary geometry in the *p*-adaptive version[2, 7, 8] are chosen as large as possible and, of course, they must avoid incompatibilities with both the geometry and the boundary conditions. So, one can understood the great significance when evaluating the integrals in (1) in order to obtain a reasonable enough accuracy. In addition, the calculation of the residual function requires the '*a-posteriori*' computation of the variables inside the boundary elements by means of equation (1), upon which the numerical integration must be carefully performed.

THE BI-CUBIC TRANSFORMATION

Let the integral

$$I = \text{⨍}\!\!\!\!-_a^b \frac{x - x_s}{|x - x_s|^\alpha} \cdot w(x) f(x)\, dx \tag{3}$$

$$x_s \in (a, b)$$

$$\alpha \in \{\mathbb{R}^+\},\ \alpha \geqslant 2$$

where ⨍ denotes 'finite part integral', $f(x)$ is any regular function differentiable enough in $[a, b]$, $w(x)$ is an arbitrary weighting function also defined in $[a, b]$ and x_s is the singular point. Assume that $f(x) \neq 0$, and if $\alpha = 2$, then integral (3) exists in the CPV sense. In the case of $\alpha \geqslant 2$, $f(x)$ needs to meet some additional conditions[17, 20] in order to be considered a 'generalized principal value integral'. In the following discussion, we shall restrict ourselves to the case $\alpha = 2$, although the proposed algorithm is also applicable even when $\alpha \geqslant 2$.

Thus, integral (3) could be rewritten as[17]

$$I = \lim_{\varepsilon \to 0^+} \left[\int_a^{x_s - \varepsilon} g(x)\, dx + \int_{x_s + \varepsilon}^b g(x)\, dx \right] \tag{4}$$

where the kernel $g(x)$ now contains the singularity of order α,

$$g(x)=\frac{x-x_s}{|x-x_s|^{\alpha}}\,w(x)f(x) \tag{5}$$

Integral (4) must be mapped into a domain $\eta\in[-1, 1]$ in order to properly perform its numerical evaluation by means of standard Gauss–Legendre quadratures. So, expression (5) becomes

$$I=\lim_{\varepsilon\to 0^+}\left[\int_{-1}^{\eta_s-\varepsilon} G(\eta)\,d\eta+\int_{\eta_s+\varepsilon}^{1} G(\eta)\,d\eta\right] \tag{6}$$

where now η_s is the image of the singularity x_s. By assuming that $w(x)=1$, it is possible to rewrite expression (5) as

$$G(\eta)=\frac{\eta-\eta_s}{|\eta-\eta_s|^{\alpha}}f(\eta)J(\eta) \tag{7}$$

where $J(\eta)$ is the Jacobian.

The central idea of the numerical procedure proposed here is based on the following two requirements:

(i) it is advisable to gather the sampling points nearby the singularity in order to improve the numerical representation of the high gradients; and
(ii) it is necessary to obtain a sampling point distribution which essentially respects the demands of equation (6), i.e. the quantity ε must be the same at both sides of the singularity η_s.

A non-linear co-ordinate transformation which satisfies requirement (i) has been proposed in Reference 27. Such a transformation works well in the case where the singular point is centred on the interval of integration ($\eta_s=0$) by reason of the symmetry of the standard Gauss–Legendre quadrature. However, when the singularity is not centred at the interval of integration ($\eta_s\neq 0$) the aforementioned transformation does not satisfy requirement (ii), thus leading to an inaccurate result.

For the sake of clarity and with no loss of generality, consider the simplest case, i.e. $f(\eta)=1$. Thus, expression (6) could be rewritten as

$$I=\lim_{\varepsilon\to 0^+}\left[\int_{-1}^{\eta_s-\varepsilon}\frac{\eta-\eta_s}{|\eta-\eta_s|^{\alpha}}\,d\eta+\int_{\eta_s+\varepsilon}^{1}\frac{\eta-\eta_s}{|\eta-\eta_s|^{\alpha}}\,d\eta\right] \tag{8}$$

Figure 1 shows the behaviour of the singular kernel in equation (8).

It is clearly understood that if requirement (ii) is not properly satisfied, the undesirable condition $|\varepsilon_a|\neq|\varepsilon_b|$ will arise and unreliable results will be obtained.

In the bi-cubic transformation proposed, the position of the sampling points is modified according to two cubic functions (hence the name bi-cubic) which are defined over both sides of the singularity. Thus, two polynomials are introduced:

$$\eta_a(\xi)=A_a\xi^3+B_a\xi^2+C_a\xi+D_a \tag{9}$$

$$\eta_b(\xi)=A_b\xi^3+B_b\xi^2+C_b\xi+D_b \tag{10}$$

where the suffix 'a' now denotes the previous region (to the singularity) of the interval of integration, whereas suffix 'b' denotes the latter region. The following boundary conditions are found to be necessary:

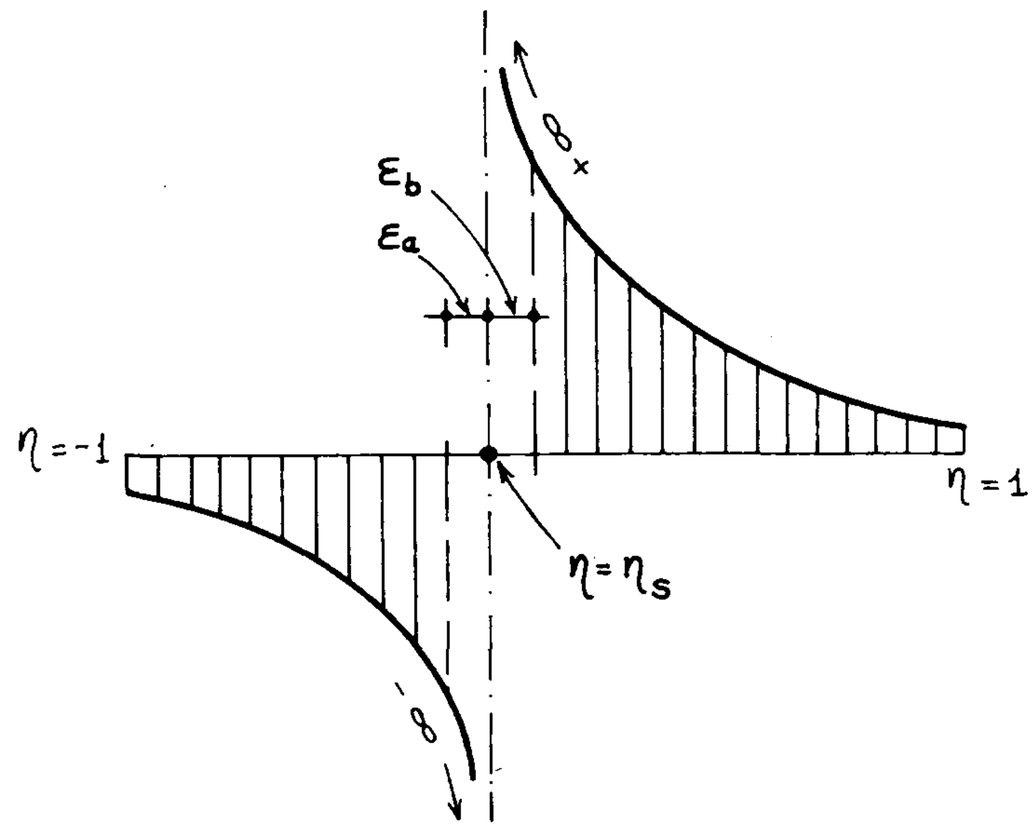

Figure 1. Singular kernel behaviour of the CPV integral

(i) previous region

$$\eta_a(\xi=-1)=-1 \tag{11}$$

$$\eta_a(\xi=1)=\eta_s \tag{12}$$

$$\eta_a(\xi_1)=\eta_s-\varepsilon \tag{13}$$

$$\left.\frac{d\eta_a}{d\xi}\right|_{\xi=1}=0 \tag{14}$$

(ii) latter region

$$\eta_b(\xi=-1)=\eta_s \tag{15}$$

$$\eta_b(\xi=1)=1 \tag{16}$$

$$\eta_b(\xi_f)=\eta_s+\varepsilon \tag{17}$$

$$\left.\frac{d\eta_b}{d\xi}\right|_{\xi=-1}=0 \tag{18}$$

As can be seen, restraints (11), (12) and (15), (16) impose, respectively, the new integration bounds for both the previous and the latter region. Restriction (13) forces the image of the last point (ξ_l) in the Gaussian quadrature used in the previous part (see Figure 2) to be placed at a distance ε from the singular point. In the same way, the image of the first point (ξ_f) in the Gaussian quadrature for the latter part is forced to be placed at a distance ε from the singular point. As a consequence, the nearly infinite values which normally occur when evaluating the singular kernel at points $\eta_s+\varepsilon$ and $\eta_s-\varepsilon$ will display the same numerical value and opposite sign, thus being conveniently cancelled. Restraints (14) and (18) smooth out the singularity near the singular point and, therefore, even better accuracy is reached. Figure 2 shows the effect that transformations (9) and (10) produce over a standard Gauss–Legendre quadrature distribution of sampling points.

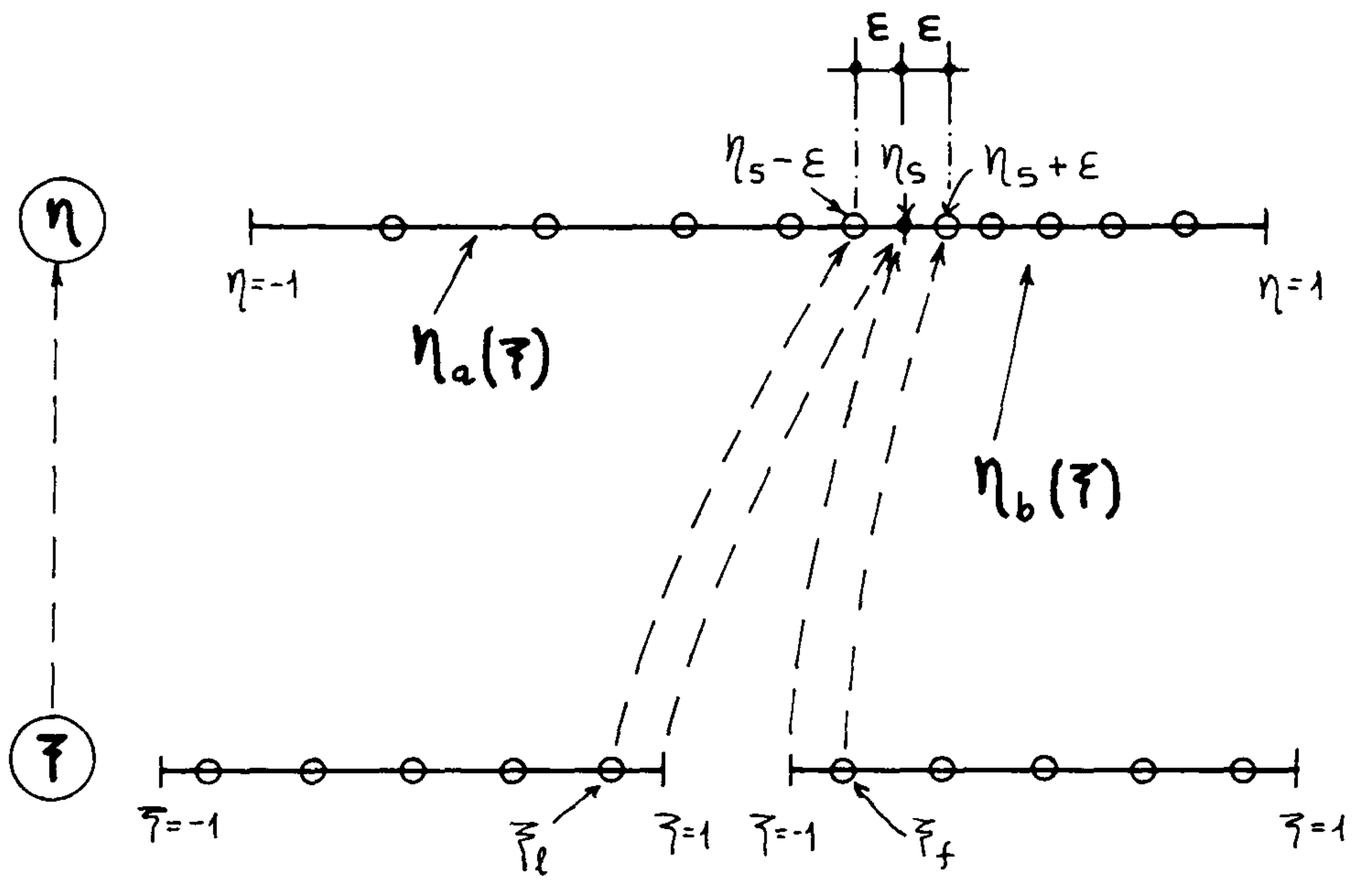

Figure 2. New distribution of sampling points produced by the bi-cubic transformation

The application of the previous boundary conditions to equations (9) and (10) yields the following values for the polynomial coefficients:

$$\left.\begin{aligned} A_a &= \frac{1+\eta_s-\varepsilon+\dfrac{1+\eta_s}{4}(\xi_1^2-1)-\dfrac{1+\eta_s}{2}(\xi_1+1)}{\xi_1^3-\xi_1^2-\xi_1+1} \\ B_a &= \frac{4A_a+1+\eta_s}{4} \\ C_a &= \frac{1+\eta_s}{2}-A_a \\ D_a &= -1+A_a-B_a+C_a \end{aligned}\right] \tag{19}$$

$$\left.\begin{aligned} A_b &= \frac{\varepsilon-\dfrac{1-\eta_s}{4}(\xi_f^2-1)-\dfrac{1-\eta_s}{2}(\xi_f+1)}{\xi_f^3+\xi_f^2-\xi_f-1} \\ B_b &= \frac{4A_b+1-\eta_s}{4} \\ C_b &= \frac{1-\eta_s}{2}-A_b \\ D_b &= 1-A_b-B_b-C_b \end{aligned}\right] \tag{20}$$

and, of course

$$J_a(\xi)=\frac{d\eta_a}{d\xi}=3A_a\xi^2+2B_a\xi+C_a \tag{21}$$

$$J_b(\xi)=\frac{d\eta_b}{d\xi}=3A_b\xi^2+2B_b\xi+C_b \tag{22}$$

Thus, if we have an integral of the form

$$I = \int_{-1}^{1} f(\eta)\, \mathrm{d}\eta \tag{23}$$

containing a singular point $\eta_s \in (-1, 1)$, its numerical evaluation by means of the bi-cubic transformation will be as follows:

$$I = \int_{-1}^{1} [f[\eta_a(\xi)]J_a(\xi) + f[\eta_b(\xi)]J_b(\xi)]\, \mathrm{d}\xi$$

$$= \sum_{k=1}^{\mathrm{NGP}} [f[\eta_a(\xi_k)]J_a(\xi_k) + f[\eta_b(\xi_k)]J_b(\xi_k)]w_k \tag{24}$$

where the ξ_k and the w_k are the abscissas and the weighting factors of the Gaussian quadrature[26] of order NGP. The use of the same order of quadrature in both the previous and the latter regions of the interval of integration is implicit in equation (24). This particularity, even though it is not binding since it is perfectly possible to use different orders, has been shown to be highly efficient and simplifies the computational details. Also investigated and developed were other non-linear transformations of higher order (up to 5). Even though acceptable results were obtained, a certain loss of accuracy is observed due to the strong gradients displayed by these functions in the neighbourhood of the singularity, thus leading to a certain shifting of the new weighting factors from the desired nearly zero value.[5]

On the other hand, our experience has shown that a numerical value of the parameter ε (see equations (19) and (20)) approximately equal to one thousandth the size of the interval of integration gives results accurate enough for practical applications in *p*-adaptive BIEM.

Another subject that should be mentioned deals with the new position of the sampling points $\eta(\xi)$ once the transformation has been done. It should be noted that the parameter ε directly affects coefficients (19) and (20) and, therefore, the behaviour of the transformation itself. As shown in Figure 3, for certain values of ε and high orders of Gaussian quadrature it may happen that some new sampling points lie outside the interval of integration.

Nevertheless, this fact does not create any limitation since it is assumed that $f(\eta)$ is analytically defined. This particularity of the bi-cubic transformation necessarily implies that some new weighting factors may also be negative, which agrees with the well-known theories of orthogonal polynomials[18, 20] from which, if the weighting functions are positively defined over the whole interval, all the integration points must lie inside the region of integration. However, 'no theorem is yet known which forces the sampling points to be contained inside the interval of integration'.[18] Moreover, if the weighting function is not positively defined over the whole interval, then the roots of the orthogonal polynomials may even be complex. Such cases, either roots lying outside the interval or complex roots, can be seen in Kutt's quadratures for orders 1, 4/3, 3/2, . . . and 2, 4, . . . , respectively.

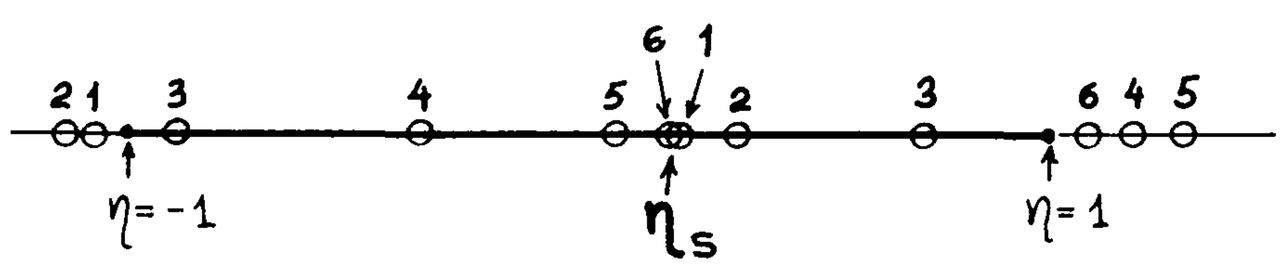

Figure 3. Particular case of new sampling points lying outside the interval of integration: $\varepsilon = 0{\cdot}003$; NGP = 6

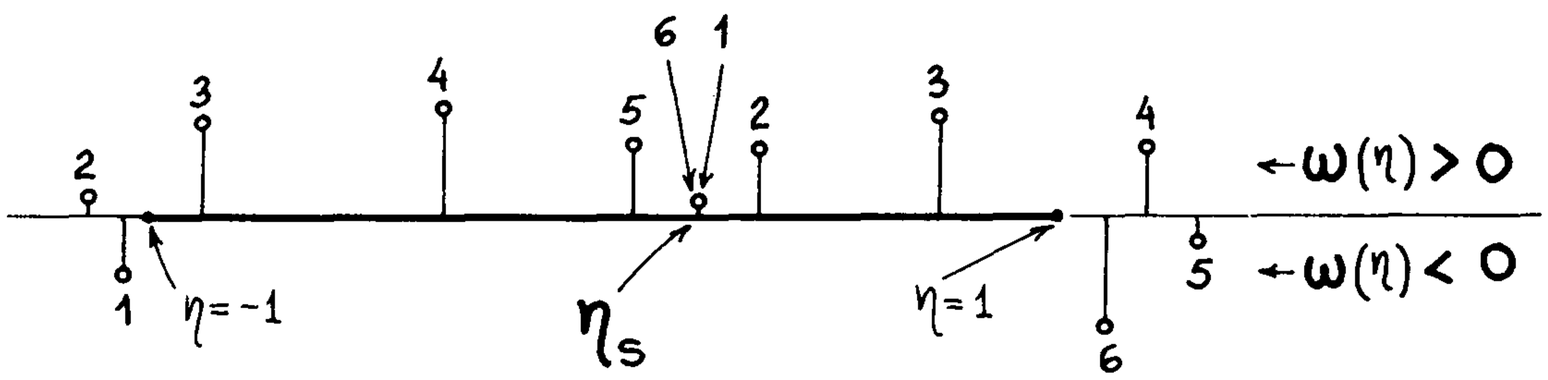

Figure 4. Particular case of negative new weighting factors: $\varepsilon=0{\cdot}003$; NGP$=6$

Thus, Figure 4 illustrates a particular situation in which some new weighting factors produced by the bi-cubic transformation are negative, in correspondence with the case of some sampling points lying outside the interval of integration (see Figure 3).

The source point coincides with one end of the element

As is well known, inaccurate results are obtained if two boundary elements of very different sizes are defined meeting a common source point and if no special precautions are taken regarding the integration procedure.

In Figure 5(a) it can be noted that if we do not appropriately satisfy the condition $|d_k|=|d_j|$, a very strong numerical contribution will normally exist at source point P which will lead to unstable results. However, the bi-cubic transformation can also be used in such a case, since it is represented by a CPV integral extended over two boundary elements. Thus, when dealing with these situations either equation (9) or equation (10) should be applied, depending upon the position of the singular point η_s, i.e.:

if $\eta_s=-1$	then use expression (10)
if $\eta_s=1$	then use expression (9)

In order to get the same d-values (see Figure 5(b)) around the source point P, the following procedure is suggested.

1. Compute an ε_k related to the smallest element meeting the source point (usually $\varepsilon_k=L_k/1000$).
2. Compute another ε_j related to the largest element meeting the source point, in such a way to ensure that $|d_k|=|d_j|$ in the real space.

These operations are rather trivial on a computer and can also be added quickly to any existing BEM code. In the same way, expressions (9) and (10) can be easily embodied into operative

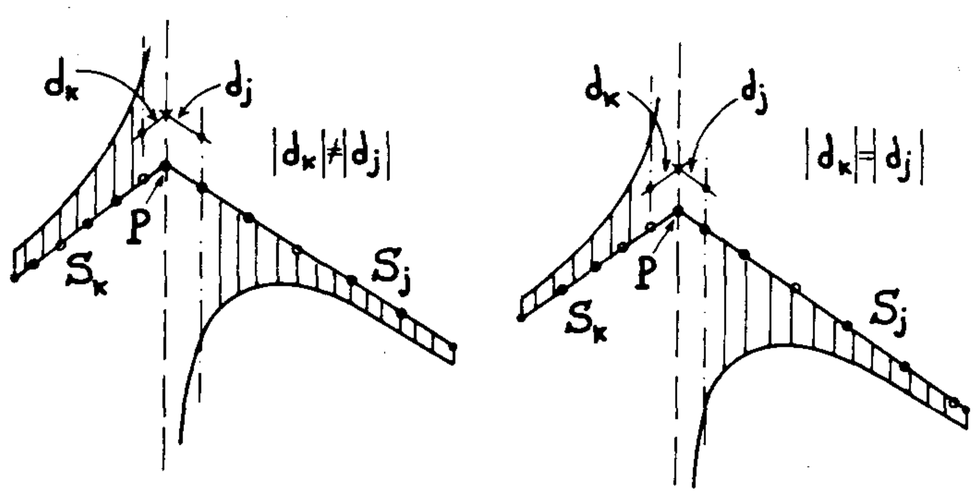

Figure 5. Boundary elements of different sizes meeting a common source point

numerical integration routines. The increment in computer time is negligible when compared with traditional schemes based upon standard Gauss–Legendre quadratures.

On the other hand, the bi-cubic transformation could be used in integration contexts other than BEM by simply adjusting the parameter ε and/or by using proper orders of integration in Gaussian quadratures.

NUMERICAL EXAMPLES

Some numerical examples, which include singularities of order $O(\log x)$, $O(1/x^{\alpha})$ and of practical application in p-adaptive BEM are included herein in order to show the great accuracy obtained by using the proposed transformation.

(i)
$$I=\int_{-1}^{1}\log|\eta-0{\cdot}8|\,d\eta \tag{25}$$

This simple example contains a singularity $O(\log x)$ at $\eta=0{\cdot}8$. Table I collects the evolution of both the numerical results as well as the errors produced (in absolute values) when using standard Gauss–Legendre quadrature, the method of Reference 27 and the bi-cubic transformation. The results are given as a function of the Gaussian quadrature order NGP.

As can be observed, satisfactory results are obtained by employing only six integration points (three in the previous region to the singularity and three in the latter one).

(ii)
$$I=\int_{-1}^{1}\frac{\operatorname{sgn}(\eta-0{\cdot}3)}{|\eta-0{\cdot}3|}\,d\eta \tag{26}$$

where sgn means 'sign of'. As in the previous case, integral (26) was evaluated by using standard Gauss–Legendre quadrature, the method of Reference 27 and the bi-cubic transformation. Table II contains both the numerical results as well as the error produced (in absolute values), as functions of the order of Gaussian quadrature NGP.

Once again, the stability and accuracy of the bi-cubic transformation can be observed. As can be seen, the method of Reference 27, that worked very well in the previous example, produces completely unacceptable results here. This kind of behaviour was the main reason to try to improve it, as discussed above, by imposing a total symmetry of the two integration points neighbouring the singular one. In this way, we enforce a numerical intepretation of the definition

Table I. Numerical evaluation of singularity $O(\log x)$

NGP	Gauss–Legendre	Gauss–Leg/Analytical	Ref. 27	Ref. 27/Analytical	Bi-cubic	Bi-cubic/Analytical
4	−1·2165E+00	+0·9625	−1·1428E+00	+0·9042	−1·4275E+00	+1·1295
6	−1·0802E+00	+0·8547	−1·2605E+00	+0·9973	−1·2757E+00	+1·0094
8	−1·7911E+00	+1·4171	−1·2762E+00	+1·0097	−1·2646E+00	+1·0006
10	−1·1442E+00	+0·9053	−1·2675E+00	+1·0028	−1·2637E+00	+0·9999
12	−1·2518E+00	+0·9904	−1·2599E+00	+0·9968	−1·2638E+00	+0·9999
14	−1·2283E+00	+0·9719	−1·2623E+00	+0·9988	−1·2638E+00	+1·0000
16	−1·1964E+00	+0·9466	−1·2652E+00	+1·0010	−1·2639E+00	+1·0000

Analytical value = −1·2638715857E+000

Table II. Numerical evaluation of singularity $O(1/x)$

NGP	Gauss–Legendre	Gauss–Leg/Analytical	Ref. 27	Ref. 27/Analytical	Bi-cubic	Bi-cubic/Analytical
4	+1·5613E+01	+25·221	+4·1241E+00	+6·662	−8·5274E+00	+13·775
6	−7·7365E+00	+12·498	+6·8693E+00	+11·097	−1·4164E+00	+2·288
8	−2·5327E+00	+4·091	+1·0711E+01	+17·302	−7·3959E−01	+1·195
10	−4·2589E−01	+0·688	+1·7129E+01	+27·670	−6·5170E−01	+1·053
12	+1·8709E+00	+3·022	+3·1865E+01	+51·475	−6·3081E−01	+1·019
14	+9·8459E+00	+15·905	+1·2227E+02	+197·509	−6·2402E−01	+1·008
16	−1·0182E+01	+16·448	−7·3087E+01	+118·065	−6·2138E−01	+1·004

Analytical value = −6·1903920841E−001

of the singularity in the CPV sense, while in the method of Reference 27 no attention is paid to the relative position of the integration points around the singularity.

(iii)
$$I = \int_{-1}^{1} \frac{\operatorname{sgn}(\eta - 0{\cdot}2)}{|\eta - 0{\cdot}2|^{1{\cdot}2}} \exp(\eta)\, d\eta \tag{27}$$

The integral shown above displays a singularity of order $\alpha = 1{\cdot}2$ at $\eta = 0{\cdot}2$ and it is included herein in order to assess the applicability of the proposed numerical procedure even when $\alpha > 1$. Table III contains both the numerical results and the errors (in absolute values) obtained by using the aforementioned methods, as functions of the order of Gaussian quadrature NGP.

As expected, numerical results show the accuracy of the bi-cubic transformation even in the presence of singularities $O(1/x^{\alpha})$ with $\alpha > 1$. Relative errors of approximately 1 per cent were obtained by employing only 10 Gauss integration points for the whole interval.

(iv) Displacement calculation on a square plate subjected to in-plane loads.

Figure 6 shows a square plate subjected to a parabolic variation of the boundary tractions. The dimensions of the domain are 100×100 cm^2, its thickness is t = 1 cm, while the Young's modulus was taken as $E = 2{\cdot}1 \times 10^6$ kgf/cm^2 and Poisson's ratio as $\nu = 0$. This problem was analysed through the p-adaptive BEM version.[5, 7] Its aim is to evaluate the displacement tensor at boundary points inside the elements in order to further calculate the residual function.

Table III. Numerical evaluation of singularity $O(1/x^{1{\cdot}2})$

NGP	Gauss–Legendre	Gauss–Leg/Finite-part	Ref. 27	Ref. 27/Finite-part	Bi-cubic	Bi-cubic/Finite-part
2	+4·9770E+00	+2·034	+6·6120E+00	+2·703	−1·1447E+02	+46·792
4	+9·9416E+00	+4·064	+1·2518E+01	+5·117	−3·6379E+00	+1·487
6	+3·0617E+01	+12·515	+2·1524E+01	+8·798	+1·8527E+00	+0·757
8	−5·7760E+01	+23·610	+3·4409E+01	+14·065	+2·3340E+00	+0·954
10	−9·3260E+00	+3·812	+5·3121E+01	+21·714	+2·4161E+00	+0·988
12	−2·5264E+00	+1·033	+8·1585E+01	+33·349	+2·4381E+00	+0·997
14	+8.4627E−01	+0·346	+1·2830E+02	+52·444	+2·4463E+00	+1·000

Finite-part (Kutt, 1975) = +2·4464143506E+000

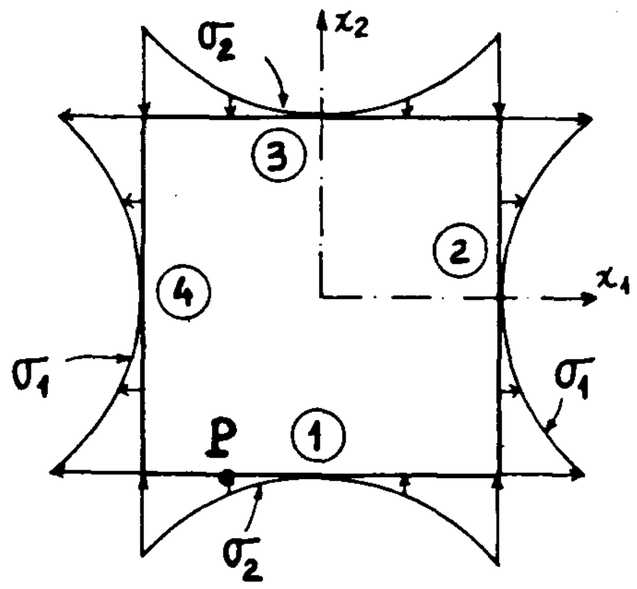

$$\sigma_1 = 2 \cdot x_2^2$$

$$\sigma_2 = -2 \cdot x_1^2$$

$$\sigma_{12} = 0$$

Figure 6. Square plate subjected to in-plane loads: boundary mesh and tractions (element numbers are encircled)

Table IV. Normalized displacements at point P. Square plate subjected to in-plane loads

NGP		Gauss–Legendre	Ref. 27	Bi-cubic	T1/T3	T2/T3
6	$\bar{u}_1$	1·0874	2·8576	0·9579	1·10	1·04
	$\bar{u}_2$	0·6503	6·4416	1·2923		
8	$\bar{u}_1$	1·0874	37·8201	0·9927	1·06	1·00
	$\bar{u}_2$	0·6503	146·2905	1·0315		
10	$\bar{u}_1$	1·0874	1·0982	0·9978	1·06	1·00
	$\bar{u}_2$	0·6503	9·3885	1·0106		
12	$\bar{u}_1$	1·0874	0·1223	0·9992	1·07	1·00
	$\bar{u}_2$	0·6503	4·5103	1·0051		
14	$\bar{u}_1$	1·0874	0·5905	0·9997	1·07	1·00
	$\bar{u}_2$	0·6503	2·6389	1·0031		
16	$\bar{u}_1$	1·0874	0·8975	1·0001	1·07	1·00
	$\bar{u}_2$	0·6503	1·4109	1·0019		

$\bar{u}_1 = u_1^{\text{COMP}}/u_1^{\text{THEORY}}$
$\bar{u}_2 = u_2^{\text{COMP}}/u_2^{\text{THEORY}}$
NGP = Number of Gauss points used on element 1
T1 = Time for standard Gauss–Legendre
T2 = Time for method of Ref. 27
T3 = Time for bi-cubic transformation

Table IV contains the displacement normalized with regards to the theoretical value at point P in element 1, as a function of the Gaussian quadrature order. Also shown is a comparison of the computer time employed by the three methods. The values obtained with the bi-cubic transformation by using 8 sampling points on element 1 and 6 sampling points on all the others (26 points for the whole boundary) are accurate enough for practical purposes in the p-adaptive BEM. The computer time is slightly less than that which corresponds to standard Gaussian quadrature, since in the latter scheme it is necessary to split the singular kernel, depending upon the type of the singularity, whereas in the bi-cubic transformation it is not.

CONCLUDING REMARKS

A new numerical procedure for the evaluation of CPV integrals and those which contain other types of singularities has been presented.

The mapping proposed herein gathers the sampling points in the neighbourhood of the singularity in order to catch the high gradients around it as in Reference 27, but uses two different third order mappings around the singularity in order to properly enforce the total symmetry of the two integration points neighbouring the singularity in the real space. As shown by the examples, that symmetry is essential for the success of the procedure.

Numerical examples have shown that the proposed method is stable and gives results accurate enough for practical applications in *p*-adaptive BEM. The formulae are rather simple. They make use of standard Gauss–Legendre quadratures and can also be quickly embodied into already existing integration routines.

On the other hand, it is not necessary to split the singular kernels which contain singularities of different orders, which notably simplifies the usual numerical procedures employed in BEM. Moreover, the formulae are capable of accurately integrating those singular functions displaying singularities of order $O(1/x^{\alpha})$, with $\alpha > 1$.

ACKNOWLEDGEMENTS

The authors wish to express their thanks for the support provided by the Consejo de Desarrollo Cientifico y Humanistico (CDCH, Venezuela) and the Instituto de Cooperacion Iberoamericana (ICI, España).